Asociación Argentina de Mecánica Computacional

Mecánica Computacional Vol XXXIII, págs. 1951-1966 (artículo completo)
Graciela Bertolino, Mariano Cantero, Mario Storti y Federico Teruel (Eds.)
San Carlos de Bariloche, 23-26 Setiembre 2014

A HALF-QUADRATIC APPROACH TO MIXED WEIGHTED SMOOTH AND ANISOTROPIC BV REGULARIZATION FOR INVERSE ILL-POSED PROBLEMS WITH APPLICATIONS TO SIGNAL AND IMAGE RESTORATION

Francisco J. Ibarrola[a] **and Ruben D. Spies**[a,b]

[a]*Departamento de Matemática, Facultad de Ingeniería Química, Universidad Nacional del Litoral, Santiago del Estero 2829, Santa Fe, Argentina, franciscoj.iba@gmail.com*

[b]*Instituto de Matemática Aplicada del Litoral, IMAL CONICET-UNL, Colectora Ruta Nacional 168, Paraje el Pozo, Santa Fe, Argentina, rspies@santafe-conicet.gov.ar*

Keywords: Inverse Problems, Ill-posedness, Regularization, Half-Quadratic

Abstract. Detection-estimation type penalizers have been widely used to regularize inverse ill-posed problems in which it is known that the solution may present discontinuities (J. Idier, Bayesian Approach to Inverse Problems, John Wiley & Sons, (2008)). For the case of quadratic penalty functionals it is known that the detection-estimation problem can be reformulated as a non-convex penalization problem. Although this approach is somewhat formally simpler, finding the corresponding global minimizer is usually a computationally challenging task, specially in high dimensional problems, such as those in image processing. At this step, a duality criterion between the non-quadratic and half-quadratic optimization becomes extremely useful to greatly reduce the computational cost (J. Idier, Convex half-quadratic criteria and interacting auxiliary variables for image restoration, IEEE Transactions on image Processing, 10(7):1001-1009, (2001)).

In this article we will consider general Tikhonov-Phillips regularization methods where the penalizers are given by mixed spatially varying weighted convex combinations of L^2 and BV functionals. Both isotropic and anisotropic BV diffusion cases will be considered. We will use the above mentioned non-convex reformulation plus a non-quadratic half-quadratic approach to attack the problem of approximating the global minimizers of those functionals. The associated optimization problems will then be recast by means of a duality argument as half-quadratic optimization problems. Numerical results in signal and image restoration problems will be shown.

1 INTRODUCTION AND PRELIMINARIES

In a general context, a linear inverse problem can be formulated as the need of finding w in an equation of the form

$$\mathcal{T}w = y, \tag{1}$$

where $\mathcal{T} : \mathcal{X} \to \mathcal{Y}$ is a bounded linear operator between two infinite dimensional Hilbert spaces $\mathcal{X}$ and $\mathcal{Y}$, the range of $\mathcal{T}$ is non-closed and y is the data, which is supposed to be known, perhaps with a certain degree of error. In the sequel and unless otherwise specified, the space $\mathcal{X}$ will be $L^2(\Omega)$ where $\Omega \subset \mathbb{R}^n$ is a bounded open convex set with Lipschitz boundary. Under these hypotheses, it turns out that problem (1) is ill-posed in the sense of Hadamard (Hadamard (1902)), the Moore-Penrose inverse of $\mathcal{T}$ is unbounded and small errors in the data y may result in very large errors in the corresponding approximations of w (Spies and Temperini (2006)). Before any attempt is made to approximate the solution of (1), the problem must be "regularized". Regularizing an inverse problem consists essentially of replacing the problem by a sequence of "well-posed" problems whose solutions converge (in an appropriate way) to a solution (or to a least squares solution) of (1). The Tikhonov-Phillips method is undoubtedly the most common way of regularizing an ill-posed problem. Although the method can be formulated within a general mathematical theory by means of spectral theory (see Engl et al. (1996)), the widespread of its use is mainly due to the fact that it can also be formulated as an unconstrained optimization problem. In fact, given an appropriate functional $P(w)$ (we shall refer to P as a penalizer in the sequel) with domain $\mathcal{D} \subset \mathcal{X}$, the regularized solution obtained by the Tikhonov-Phillips method and such a penalizer, is the global minimizer over $\mathcal{D}$, w_α, (provided it exists), of the functional

$$J_{\alpha,P}(w) = \|\mathcal{T}w - y\|^2 + \alpha P(w), \tag{2}$$

where α is a positive constant called regularization parameter. The original method was found independently by Phillips and Tikhonov in 1962 and 1963 (Phillips (1962) and Tikhonov (1963)) using $P(w) = \|w\|^2_{L^2(\Omega)}$. Other penalizers can also be used to regularize the problem. Each choice of P results in a different regularized solution possessing particular properties. In the past 15 years considerable attention has been given to finding "appropriate" penalizers for a given problem. Thus, for instance, the choice of $P(w) = \|w\|^2_{L^2(\Omega)}$ produces always smooth regularized approximations which converge, as $\alpha \to 0^+$, to the best approximate solution (i.e. the least squares solution of minimum norm) of problem (1) (see Engl et al. (1996)) while for $P(w) = \||\nabla w|\|^2_{L^2(\Omega)}$ the order-one Tikhonov-Phillips method is obtained. Similarly, the choice of $P(w) = \|w\|_{\mathrm{BV}(\Omega)}$ (where $\|\cdot\|_{\mathrm{BV}}$ denotes the total variation norm) or $P(w) = \||\nabla w|\|_{L^1(\Omega)}$, result in the so called "bounded variation regularization methods" (Acar and Vogel (1994), Rudin et al. (1992)). The use of these of penalizers is strongly suggested when preserving discontinuities or edges is an important matter. The method, however, tends to produce piecewise constant approximations and therefore it will most likely be inappropriate in regions where the exact solution is smooth (Chambolle and Lions (1997)), producing the so called "staircasing effect". For general penalizers P, sufficient conditions guaranteeing existence, uniqueness and weak and strong stability of the minimizers under different types of perturbations were found in Mazzieri et al. (2012).

Given that each penalizing term engraves the solution with particular properties, in certain types of problems, particularly in those in which it is known that the regularity of the exact solution is heterogeneous and/or anisotropic, it is reasonable to think that the use of two or more penalizers of different nature, that could somehow spatially adapt to the local characteristics of the exact solution, would be more convenient. During the last 15 years many regularization methods have been developed in light of this reasoning. Thus, for instance, in 1997 Blomgren *et al.* (Blomgren et al. (1997)) proposed the following penalizer:

$$P(w) = \int_\Omega |\nabla w|^{p(|\nabla w|)} dx, \tag{3}$$

where p is a decreasing function satisfying $\lim_{u \to 0^+} p(u) = 2$, $\lim_{u \to \infty} p(u) = 1$. Thus, in regions where the gradient of w is small the penalizer is approximately equal to $\||\nabla w|\|^2_{L^2(\Omega)}$, corresponding to a Tikhonov-Phillips method of order one (appropriate for smooth regions). On the other hand, when the modulus of the gradient of w is large, the penalizer resembles the bounded variation seminorm $\||\nabla w|\|_{L^1(\Omega)}$, which, as previously mentioned, is a good choice for border detection purposes. Although this model for P is quite reasonable, proving basic properties of the corresponding generalized Tikhonov-Phillips functional turns out to be quite difficult. The authors proved existence of global minimizers of functional (2), by using the theory of variable L^p spaces. In 1997 Chambolle and Lions suggested a different way of combining these two methods (Chambolle and Lions (1997)). They defined a thresholded penalizer of the form:

$$P_\beta(w) = \int_{|\nabla w| \leq \beta} |\nabla w|^2 \, dx + \int_{|\nabla w| > \beta} |\nabla w| \, dx,$$

where $\beta > 0$ is a prescribed threshold parameter. Thus, in regions where borders are more likely to be present ($|\nabla w| > \beta$), penalization is made with the bounded variation seminorm while a standard order-one Tikhonov-Phillips method is used otherwise. This model was shown to be successful in restoring images possessing regions with homogeneous intensity separated by borders. However, in the case of images with non-uniform or highly degraded intensities, the model is extremely sensitive to the choice of the threshold parameter β. More recently, penalizers of the form

$$P(w) = \int_\Omega |\nabla w|^{p(x)} dx, \tag{4}$$

for certain functions p with range in $[1, 2]$, were studied in Chen et al. (2006) and Li et al. (2010). It is timely to point out here that all previously mentioned results are valid only for the case of denoising (no blurring), i.e. for the case $\mathcal{T} = id$. More recently, Mazzieri, Spies and Temperini studied penalizers of the form

$$P(w) = \lambda_0 \int_\Omega |\sqrt{1 - \theta(x)}\, w(x)|^2 dx + \lambda_1 \int_\Omega \|\theta(x)\mathcal{A}(x)\nabla w(x)\| dx \tag{5}$$

where λ_0, λ_1 are positive constants, $\theta(x)$ is a weighting function with values on the interval $[0, 1]$ and $A(x)$ is a symmetric positive definite matrix field. General existence, uniqueness and stability results of global minimizers of the corresponding generalized Tikhonov-Phillips functionals

$$\mathcal{J}_\theta(w) = \|\mathcal{T}w - y\|^2 + \lambda_0 \int_\Omega |\sqrt{1 - \theta(x)}\, w(x)|^2 dx + \lambda_1 \int_\Omega \|\theta(x)\mathcal{A}(x)\nabla w(x)\| dx \tag{6}$$

can be found in Mazzieri et al. (2014b) and Mazzieri et al. (2014a). Several remarks are in order. First note that the extreme case $\theta(x) = 0$ $\forall x$ corresponds to the classical Tikhonov-Phillips method. For $\theta(x) = 1$ $\forall x$ one gets a pure BV method, with the classical Bounded Variation method corresponding to the case of $\mathcal{A}(x) = I$ $\forall x$. Other choices of the matrix field A are possible in order to induce an anisotropic BV penalization. Feasible ways of constructing this matrix field can be found for instance in Calvetti et al. (2006). The general case can then be thought of as a convex combination of a classical L^2 and an anisotropic BV penalizers.

2 SIGNAL RESTORATION WITH A HALF QUADRATIC APPROACH TO MIXED REGULARIZATION

Approximating the minimizer of (6) presents quite serious computational challenges. In fact, for high dimensional problems like those arising in image restoration, all standard optimization algorithms will require many hours of CPU time in any modern personal computer. In order to reduce the computational burden originated by this difficulty, we shall next consider an alternative approach to the problem of finding the minimizer of (6). The tactic is based upon a method developed by J. Idier in Idier (2008) for solving detection-estimation problems, and it consists of rewriting the functional in an appropriate form via half-quadratic optimization tools. To introduce this approach, we will first consider the case of minimizing functional (6) when Ω is a subset of $\mathbb{R}$, meaning $w(x)$ represents the signal we wish to restore. Without loss of generality we shall assume $\Omega = [0, 1]$. The operator $\mathcal{A}$ will necessarily be the identity, meaning our functional takes the form

$$\mathcal{J}_\theta(w) = \|\mathcal{T}w - y\|^2 + \lambda_0 \int_0^1 |\sqrt{1-\theta(x)}\, w(x)|^2 dx + \lambda_1 \int_0^1 |\theta(x) w'(x)| dx. \tag{7}$$

2.1 Signal restoration by mixed regularization

Since restoring the signal $w(x)$ is tantamount to finding the minimizer of the previous functional, we will need to perform a discretization in order to proceed numerically. For that, we will take M equally spaced points $x_m = \frac{2m-1}{2M} \in [0, 1]$, $m = 1, \ldots, M$, and define our discretized signal $u \in \mathbb{R}^M$ by $u_m \doteq w(x_m)$ for $m = 1, 2, ..., M$. In the same way, let $T \in \mathbb{R}^{N\times M}$ and $v \in \mathbb{R}^N$ be discretized versions of the operator $\mathcal{T}$ and of the observation y, respectively, and let $\theta_m \doteq \theta(x_m)$ for $m = 1, 2, ..., M$. We now introduce a discrete finite-differences approximation of functional (7) as follows:

$$J_\theta(u) = \|Tu - v\|^2 + \frac{\lambda_0}{M} \sum_{m=1}^{M} (1-\theta_m) u_m^2 + \frac{\lambda_1}{M} \sum_{m=2}^{M} \theta_m \left| \frac{u_m - u_{m-1}}{1/M} \right|. \tag{8}$$

The restored signal $w(x)$ will then be approximated by the discrete signal represented by the vector minimizing this functional. The main difficulty for finding such a minimizer arises from the non-differentiability of the absolute value at the origin, which precludes the differentiability of $J_\theta(u)$. To overcome this impediment we shall replace the absolute value by a function $\phi(t)$ approximating it and satisfying certain additional regularity and asymptotic assumptions. For general non-quadratic penalizers, in order to preserve edges and discontinuities between homogeneous regions, it is important to appropriately choose the behavior of the function ϕ. Two groups of functions have mainly been considered in the literature. Namely:

- L_2L_1: we say that a function $\phi : \mathbb{R} \to \mathbb{R}$ is of L_2L_1 class if it is even, non-constant, convex and of class $\mathcal{C}^1$ on $\mathbb{R}$, $\mathcal{C}^2$ at the origin and asymptotically linear.

- L_2L_0: we say that a function $\phi : \mathbb{R} \to \mathbb{R}$ is of L_2L_0 class if it is even, non-constant, non-decreasing on $\mathbb{R}^+$, asymptotically constant and of class $\mathcal{C}^2$ at the origin.

It is important to point out, however, that an L_2L_1 or L_2L_0 function does not need to be an approximation of the absolute value. Thus, for instance, in certain detection-estimation problems for the case of restoration of piecewise smooth signals, the L_2L_0 function $\phi(t) = \min\{t^2, \eta^2\}$

(for a given η), results appropriate (Idier (2008), Section 6.4.1). In our case, we will pick the L_2L_1 function

$$\phi(t) = \phi_\eta(t) \doteq \sqrt{t^2+\eta^2} - \eta, \tag{9}$$

for $\eta > 0$ sufficiently small, and replace functional (8) with

$$J_{\theta,\phi}(u) = \|Tu - v\|^2 + \frac{\lambda_0}{M}\sum_{m=1}^{M}(1-\theta_m)u_m^2 + \frac{\lambda_1}{M}\sum_{m=2}^{M}\theta_m \phi\left(\frac{u_m - u_{m-1}}{1/M}\right). \tag{10}$$

Now that we have a differentiable functional, we will introduce a duality relation which will later allow us to conveniently write the corresponding first order necessary condition as a linear system.

2.2 Non-quadratic and half-quadratic duality

Let $\phi(t)$ be a non-quadratic function satisfying: (i) $\phi(t)$ is even; (ii) $\phi(\sqrt{t})$ is concave on $\mathbb{R}^+$ and (iii) $\phi(t)$ is continuous at $t = 0$ and $\phi \in \mathcal{C}^1(\mathbb{R}\backslash\{0\})$. Under these hypotheses, it can be shown (Rockafellar (1970), Section 12) that there exists a function $\psi(b)$ so that the pair (ϕ, ψ) satisfy the following duality relation:

$$\phi(t) = \inf_{s>0}(st^2 + \psi(s)), \tag{11}$$

$$\psi(s) = \sup_{t\in\mathbb{R}}(\phi(t) - st^2).$$

Expression (11) is usually referred to as the half-quadratic form of ϕ. For instance, for $\phi = \phi_\eta$ as in (9), it can be easily shown that the corresponding dual function is

$$\psi_\eta(s) = \eta^2 s - \eta + \frac{1}{4s}. \tag{12}$$

By using the dual function $\psi(s)$ we now define the following functional, which introduces an auxiliary variable $s \in \mathbb{R}_+^{M-1}$:

$$\begin{aligned} K_{\theta,\phi}(u,s) \doteq & \|Tu - v\|^2 + \frac{\lambda_0}{M}\sum_{m=1}^{M}(1-\theta_m)u_m^2 \\ & + \frac{\lambda_1}{M}\sum_{m=2}^{M}\theta_m\left(s_m\left(\frac{u_m - u_{m-1}}{1/M}\right)^2 + \psi(s_m)\right). \end{aligned} \tag{13}$$

Functional (13) is strongly rooted in the origin of the detection-estimation formalism, where an additional variable is used to define an augmented criterion to take possible discontinuities into account. It turns out that functionals (10) and (13) are closely related. In fact, by minimizing $K_{\theta,\phi}(u,s)$ with respect to $s \in \mathbb{R}_+^{M-1}$ we obtain:

$$\begin{aligned} & \inf_{s\in\mathbb{R}_+^{M-1}} K_{\theta,\phi}(u,s) \\ = & \|Tu - v\|^2 + \frac{\lambda_0}{M}\sum_{m=1}^{M}(1-\theta_m)u_m^2 + \frac{\lambda_1}{M}\inf_{s\in\mathbb{R}_+^{M-1}}\left[\sum_{m=2}^{M}\theta_m\left(s_m\left(\frac{u_m - u_{m-1}}{1/M}\right)^2 + \psi(s_m)\right)\right] \end{aligned}$$

$$
\begin{aligned}
=&\|Tu-v\|^2+\frac{\lambda_0}{M}\sum_{m=1}^{M}(1-\theta_m)u_m^2+\frac{\lambda_1}{M}\sum_{m=2}^{M}\theta_m\inf_{s_m\in\mathbb{R}_+}\left(s_m\left(\frac{u_m-u_{m-1}}{1/M}\right)^2+\psi(s_m)\right)\\
=&\|Tu-v\|^2+\frac{\lambda_0}{M}\sum_{m=1}^{M}(1-\theta_m)u_m^2+\frac{\lambda_1}{M}\sum_{m=2}^{M}\theta_m\phi\left(\frac{u_m-u_{m-1}}{1/M}\right)\\
=&J_{\theta,\phi}(u),
\end{aligned}
\tag{14}
$$

where the second equality holds since each element of s is associated independently to one and only one term of the sum. By defining a diagonal matrix $B\in\mathbb{R}^{M\times M}$, with diagonal elements b_m such that $b_1=0$, and $b_m=\underset{s_m\in\mathbb{R}_+}{\arg\min}\left(s_m\left(\frac{u_m-u_{m-1}}{1/M}\right)^2+\psi(s_m)\right)$ for $m=2,3,...,M$ (assuming those minimizers do exist) and using identity (14), we can then write

$$
J_{\theta,\phi}(u)=\|Tu-v\|^2+\frac{\lambda_0}{M}\sum_{m=1}^{M}(1-\theta_m)u_m^2+\frac{\lambda_1}{M}\sum_{m=2}^{M}\theta_m\left(b_m\left(\frac{u_m-u_{m-1}}{1/M}\right)^2+\psi(b_m)\right).
$$

Furthermore, if we define the diagonal matrix $\Theta\in\mathbb{R}^{M\times M}$ by $\Theta_{m,m}=\theta_m$ and we let L_1 be the one-dimensional first order finite difference matrix (i.e. $(L_1u)_m=u_m-u_{m-1}$ for $m=2,3,...,M$ and $L_{1,1}=0$), we can finally write

$$
J_{\theta,\phi}(u)=\|Tu-v\|^2+\frac{\lambda_0}{M}u^t(I_M-\Theta)u+\lambda_1Mu^tL_1^t\Theta BL_1u+\frac{\lambda_1}{M}\sum_{m=2}^{M}\theta_m\psi(b_m). \tag{15}
$$

Finding the minimizer of $J_{\theta,\phi}(u)$ is now, in principle, a simple task. In fact, by using expression (15), the first order necessary condition leads to the (apparently) linear system

$$
(T^tT+\frac{\lambda_0}{M}(I_M-\Theta)+\lambda_1ML_1^t\Theta BL_1)u=T^tv. \tag{16}
$$

It is important no note, nonetheless, that the diagonal elements b_m of matrix B depend on u and hence, strictly speaking, (16) is in general a non-linear system. Here again, the duality relation comes in handy since by differentiating expression (11) we observe that the elements b_m must satisfy

$$
b_m=\frac{\phi'(t_m)}{2t_m}, \tag{17}
$$

where $t_m=(u_m-u_{m-1})/(1/M)$. Let us notice that $\phi(t)$ has continuous second order derivative at zero, provided that $\phi(t)$ be of class L_2L_1 or L_2L_0. Thus, ϕ has finite second order derivative at $t=0$, and then L'Hôpital's rule implies that $\frac{\phi'(t)}{2t}$ has a removable singularity at zero. Hence for $t_m=0$, we define $b_m=\phi''(0)/2$.

We shall now proceed to build an algorithm for approximating the minimizer of $J_{\theta,\phi}(u)$ by using expressions (16) and (17) via a fixed-point type argument as follows.

2.3 Numerical implementation of the half-quadratic approach

Since minimizing (15) implies the simultaneous minimization with respect to the inter-dependent variables u_m and b_m, we will state a simple cyclic iterative algorithm that was found to be quite effective:

Step 1 - Initializing: set $j = 0$, and initialize $u^j = u^0$.

Step 2 - Counting: let $j = j + 1$.

Step 3 - Updating B**:** update the components b^j_m of B^j using equation (17). That is,

$$b^j_m \doteq \frac{\phi'(M(u^{j-1}_m - u^{j-1}_{m-1}))}{2M(u^{j-1}_m - u^{j-1}_{m-1})}.$$

Step 4 - Updating $\mathbf{u}$**:** update u^j by solving (in the least-squares sense) the linear system

$$(T^tT + \frac{\lambda_0}{M}(I_M - \Theta) + \lambda_1 M\Theta L_1^t B^j L_1)u^j = T^t v.$$

Step 5 - Convergence: if a previously defined convergence criterion is satisfied, the algorithm ends and the restored signal is defined to be u^j. Else, the algorithm repeats from step 2.

Remark: clearly several convergence stopping criteria can be used in Step 5 above. Here and in all the examples that follow this was: stop whenever $|\delta_j - \delta_{j-1}| < \alpha$, where δ_j is the parameter value of Morozov's discrepancy principle corresponding to u_j and α is a sufficiently small parameter. In our case we took $\alpha = 10^{-5}$.

In the next section, we shall generalize this half-quadratic approach to the case of image restoration problems (i.e. for $n = 2$).

3 THE HALF-QUADRATIC APPROACH TO IMAGE RESTORATION WITH MIXED L^2 AND ANISOTROPIC BV REGULARIZATION

Consider now the model problem (1) along with functional (6) and assume $\Omega = [0,1]\times[0,1]$. Here now $w(x)$ represents the intensity of a gray-scale image at the point $x \in \Omega$. We discretize the image to obtain an M-by-M matrix U, consisting of the values of w at the centerpoints of an M-by-M pixel grid. Next, we stack the columns of U to get a vector $u \in \mathbb{R}^{M^2}$ so that $u_{M(l-1)+m} = U_{m,l}\ \forall\, l,m = 1,2,...,M$. We proceed in the same way to obtain $\Theta \in \mathbb{R}^{M^2}$ and $v \in \mathbb{R}^{N^2}$, corresponding to discretized versions of $\theta(\cdot)$ and the observation y, respectively. Finally, $T \in \mathbb{R}^{N^2\times M^2}$ will represent an appropriately discretized version of the operator $\mathcal{T}$ and A_m the 2-by-2 matrix obtained by evaluating the matrix-valued function $\mathcal{A}(\cdot)$ at the centerpoint of the m^{th} pixel. Thus, our discretization of functional (6) takes the form

$$J_\theta(u) = \|Tu-v\|^2 + \frac{\lambda_0}{M^2}\sum_{m=1}^{M^2}(1-\theta_m)u_m^2 + \frac{\lambda_1}{M^2}\sum_{m\in\mathfrak{M}}\theta_m \left\| A_m \begin{pmatrix} M(u_m - u_{m+1}) \\ M(u_m - u_{m-M}) \end{pmatrix} \right\|_1, \quad (18)$$

where $\mathfrak{M}$ is the set of all indexes which do not correspond to a pixel in the bottom or left borders of the image. Naturally, the restored image will be approximated by the minimizer of this functional. In order to find such a minimizer, let us begin by noticing that the m-th term of the discretized anisotropy penalizer on (18) is now

$$\begin{aligned}\left\| A_m \begin{pmatrix} M(u_m - u_{m+1}) \\ M(u_m - u_{m-M}) \end{pmatrix} \right\|_1 &= \left| M\left(a^m_{1,1}(u_m - u_{m-M}) + a^m_{1,2}(u_m - u_{m+1})\right) \right| \\ &+ \left| M\left(a^m_{2,1}(u_m - u_{m-M}) + a^m_{2,2}(u_m - u_{m+1})\right) \right|, \quad (19)\end{aligned}$$

where $a^m_{i,j}$, $i,j = 1,2$, are the elements of the 2-by-2 matrix A_m. Here again, to avoid the non-differentiability at the origin of the absolute value, we will replace it with the function $\phi(t) = \phi_\eta(t)$ defined in (9), for which the corresponding dual is function $\psi(s) = \psi_\eta(s)$ given in (12). Following the same steps as in section 3.2 and using the duality relation (11), we approximate (19) by

$$\left\| A_m \begin{pmatrix} M(u_m - u_{m+1}) \\ M(u_m - u_{m-M}) \end{pmatrix} \right\|_1 \approx b_m \left[M \left(a^m_{1,1}(u_m - u_{m-M}) + a^m_{1,2}(u_m - u_{m+1}) \right) \right]^2 + \psi(b_m) \\ + c_m \left[M \left(a^m_{2,1}(u_m - u_{m-M}) + a^m_{2,2}(u_m - u_{m+1}) \right) \right]^2 + \psi(c_m), \tag{20}$$

where

$$b_m \doteq \underset{s_m \in \mathbb{R}_+}{\arg\min} \left(s_m M^2 \left(a^m_{1,1}(u_m - u_{m-M}) + a^m_{1,2}(u_m - u_{m+1}) \right)^2 + \psi(s_m) \right),$$

and

$$c_m \doteq \underset{s_m \in \mathbb{R}_+}{\arg\min} \left(s_m M^2 \left(a^m_{2,1}(u_m - u_{m-M}) + a^m_{2,2}(u_m - u_{m+1}) \right)^2 + \psi(s_m) \right).$$

Define now the M^2-by-M^2 diagonal matrices $A^{i,j}$ for $i,j = 1,2$, such that $A^{i,j}_{m,m} = a^m_{i,j}$ if $m \in \mathfrak{M}$ and $A^{i,j}_{m,m} = 0$ otherwise, and let R_1 and R_2 be the M^2-by-M^2 matrices defined by $R_1 \doteq A^{1,1}(L_1 \otimes I_M) + A^{1,2}(I_M \otimes L_1^t)$ and $R_2 \doteq A^{2,1}(L_1 \otimes I_M) + A^{2,2}(I_M \otimes L_1^t)$, where I_M denotes the M-th indentity matrix and $\otimes$ is the Kronecker product. It is then easy to see that, using (20), functional (18) can be approximated by

$$J_{\theta,\phi}(u) = \|Tu - v\|^2 + \frac{\lambda_0}{M^2} u^t (I_{M^2} - \Theta) u + \lambda_1 u^t R_1^t \Theta B R_1 u + \lambda_1 u^t R_2^t \Theta C R_2 u \\ + \frac{\lambda_1}{M^2} \sum \theta_m \psi(b_m) + \frac{\lambda_1}{M^2} \sum \theta_m \psi(c_m), \tag{21}$$

where B and C are the M^2-by-M^2 diagonal matrices whose diagonal elements are b_m and c_m, respectively. We now want to find the minimizer of functional (21). As for the case of signals (equation (15)), this seems to be a relatively easy task. In fact, once again the first order necessary condition resembles a linear system and is given by

$$\left(T^t T + \frac{\lambda_0}{M^2} (I_{M^2} - \Theta) + \lambda_1 R_1^t \Theta B R_1 + \lambda_1 R_2^t \Theta C R_2 \right) u = T^t v. \tag{22}$$

We should observe, however, that matrices B and C depend on u and system (22) is in fact nonlinear. Nevertheless, differentiation of the duality relation (11) implies that the diagonal elements b_m and c_m of those matrices must satisfy

$$b_m = \frac{\phi'\left(M \left(a^m_{1,1}(u_m - u_{m-M}) + a^m_{1,2}(u_m - u_{m+1}) \right)\right)}{2M \left(a^m_{1,1}(u_m - u_{m-M}) + a^m_{1,2}(u_m - u_{m+1}) \right)} \tag{23}$$

and

$$c_m = \frac{\phi'\left(M \left(a^m_{2,1}(u_m - u_{m-M}) + a^m_{2,2}(u_m - u_{m+1}) \right)\right)}{2M \left(a^m_{2,1}(u_m - u_{m-M}) + a^m_{2,2}(u_m - u_{m+1}) \right)}. \tag{24}$$

Based upon all of the above, we shall state a cyclic iterative algorithm for image restoring as follows:

Step 1 - Initializing: set $j = 0$, and initialize $u^j = u^0$.

Step 2 - Counting: let $j = j + 1$.

Step 3 - Updating B: update the components b^j_m of B^j using equation (23). That is,

$$b^j_m = \frac{\phi'(M\left(a^m_{1,1}(u^{j-1}_m - u^{j-1}_{m-M}) + a^m_{1,2}(u^{j-1}_m - u^{j-1}_{m+1})\right))}{2M\left(a^m_{1,1}(u^{j-1}_m - u^{j-1}_{m-M}) + a^m_{1,2}(u^{j-1}_m - u^{j-1}_{m+1})\right)}$$

Step 4 - Updating C: update the components c^j_m of C^j using equation (24). That is,

$$c^j_m = \frac{\phi'(M\left(a^m_{2,1}(u^{j-1}_m - u^{j-1}_{m-M}) + a^m_{2,2}(u^{j-1}_m - u^{j-1}_{m+1})\right))}{2M\left(a^m_{2,1}(u^{j-1}_m - u^{j-1}_{m-M}) + a^m_{2,2}(u^{j-1}_m - u^{j-1}_{m+1})\right)}$$

Step 5 - Updating u: update u^j by solving the linear system

$$\left(T^tT + \frac{\lambda_0}{M^2}(I_{M^2} - \Theta) + \lambda_1 R_1^t \Theta B^j R_1 + \lambda_1 R_2^t \Theta C^j R_2\right) u^j = T^t v$$

Step 6 - Convergence: if the convergence criterion is satisfied, the algorithm ends and our restored signal is defined as u^j. Else, the algorithm repeats from step 2.

4 APPLICATIONS TO SIGNAL AND IMAGE RESTORATION

The purpose of this section is to present some applications of the algorithms developed above for half-quadratic mixed L^2-BV regularization in signal and image restoration problems.

4.1 A signal restoration example

A basic mathematical model for signal blurring is given by convolution, as a Fredholm integral equation of first kind:

$$y(x) = \int_0^1 k(t,x)w(t)dt \doteq \mathcal{T}w(x), \tag{25}$$

where $k(t,x) = \frac{1}{\sqrt{2\pi}\sigma_b}\exp\left(-\frac{(t-x)^2}{2\sigma_b^2}\right)$ is a Gaussian kernel, $\sigma_b > 0$, w is the original signal and y is the blurred signal. For the numerical examples that follow, equation (25) was discretized in the usual way (using collocation and quadrature), resulting in a discrete model of the form

$$Tu = v, \tag{26}$$

where T is a $(M+1)\times(M+1)$ matrix, $u, v \in \mathbb{R}^{M+1}$ ($u_j = w(x_j)$, $v_j = y(x_j)$, $x_j = \frac{j}{M}$, $0 \leq j \leq M$). We took $M = 130$ and $\sigma_b = 0.04$. The data g was contaminated with a 1.5% zero-mean Gaussian additive noise (i.e. standard deviation equal to 1.5% of the range of v). Figure 1(a) shows the original signal u (unknown in real life problems) and the blurred noisy signal v which constitutes the data of the inverse problem. Figure 1(b) shows the restoration obtained with the classical Tikhonov-Phillips method (corresponding to $\theta(x) = 0$ in functional (6)). Figure 1(c) shows the restoration obtained with the pure BV penalizer ($\theta(x) = 1$ in (6)) and finally, Figure 1(d) depicts the restoration obtained with the mixed L^2-BV penalizer with $\theta(x)$

chosen by scaling to [0,1] the modulus of the gradient of the regularized solution obtained with a pure Tikhonov-Phillips method. It is timely to point out here that the choice of the function θ is a very important matter which we do not discuss in this article. In all cases, the regularization parameters used (λ_0 and λ_1) were estimated using Morozov's discrepancy principle. The actual values of these parameters for all examples that follow are shown on Table 3 at the end of this article.

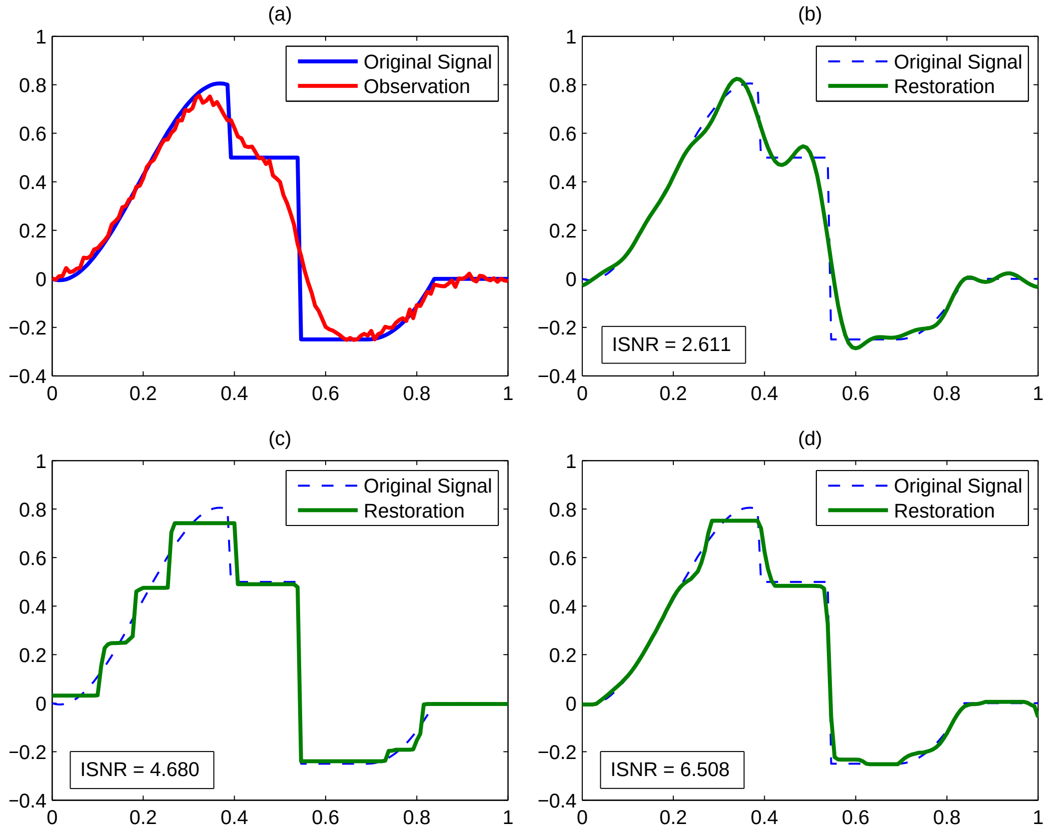

Figure 1: (a) Original signal and observation; (b) Tikhonov-Phillips restoration; (c) BV restoration; (d) Mixed L^2-BV restoration.

As expected, the combined method returns a much better restoration. This is clearly reflected in the ISNRs for all three cases. The CPU times required to perform the latter mixed restoration was compared to those required by another program based in the traditional Newton-Raphson method. Given the same stopping criteria, the algorithm proposed here was in average over thirty five times faster than the other, what provides strong evidence of the computational efficiency of these new half-quadratic approach. We will next present an application to an image restoration problem, of the method and algorithm developed in Section 3.

4.2 Image restoration examples

4.2.1 A gray-scale image

For the following examples we used a two dimensional convolution model for the blurring operator with point spread function (PSF) of atmospheric turbulence type (gaussian kernel) with vertical and horizontal variances σ_v^2 and σ_h^2, respectively:

$$\mathcal{T}w(x,y) = \int\int_{\Omega} (2\pi\sigma_h\sigma_v)^{-1} \exp\left(-\frac{(x-s)^2}{2\sigma_h^2} - \frac{(y-t)^2}{2\sigma_v^2}\right) w(s,t)\, ds\, dt. \qquad (27)$$

Here $w(s,t)$, for $(s,t) \in \Omega \subset \mathbb{R}^2$, represents the gray-scale intensity at the point (s,t) of the image we want to restore. The set Ω is the support of the image, which in all cases we take to be $[0,1] \times [0,1]$. Here too, model (27) was discretized in the usual way by taking a regular $M \times M$ grid on Ω and stacking the columns of the discretized version of the image $w(s,t)$ to form a vector $u \in \mathbb{R}^{M^2}$. The resulting discretized model is then of the form $Tu = v$ where T is an M^2-by-M^2 matrix and the components of v correspond to the values of the observation $\mathcal{T}w(x,y)$ at the centerpoints of the corresponding pixels. For the examples that follow we took $\sigma_v^2 = \sigma_h^2 = 0.02$, $M = 100$ and the data of the inverse problem (namely v) was contaminated with 1% additive zero mean Gaussian noise.

Figure 2(a) shows the blurred-noisy image (data of the inverse problem) while Figure 2(b) shows the restoration obtained with a Tikhonov-Phillips method (pure L^2 penalizer). This restoration was later used to build the anisotropic penalization matrices A_m and the components θ_m of the convex combination vector. In the following examples, the elements θ_m were computed by scaling to $[0,1]$ the norm of the discretized gradient of the pure Tikhonov-Phillips solution. As for the matrices A_m, they were constructed following the theory in Calvetti et al. (2006) (for reasons of brevity we do not give further details here).

(a) (b)

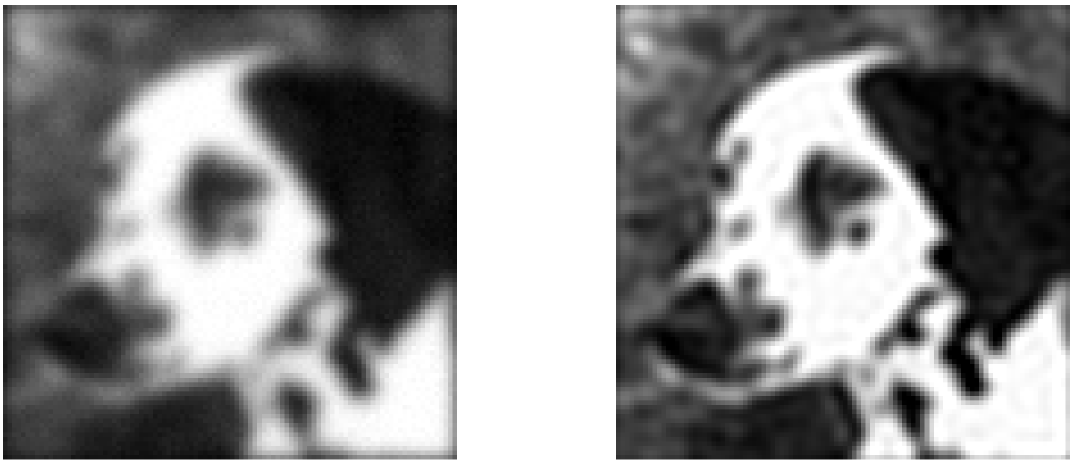

Figure 2: (a) Blurred noisy image (observation); (b) Tikhonov-Phillips restoration.

In Figure 3 we present the restorations obtained using pure BV penalizers; isotropic case in (a) and anisotropic in (b).

(a) (b)

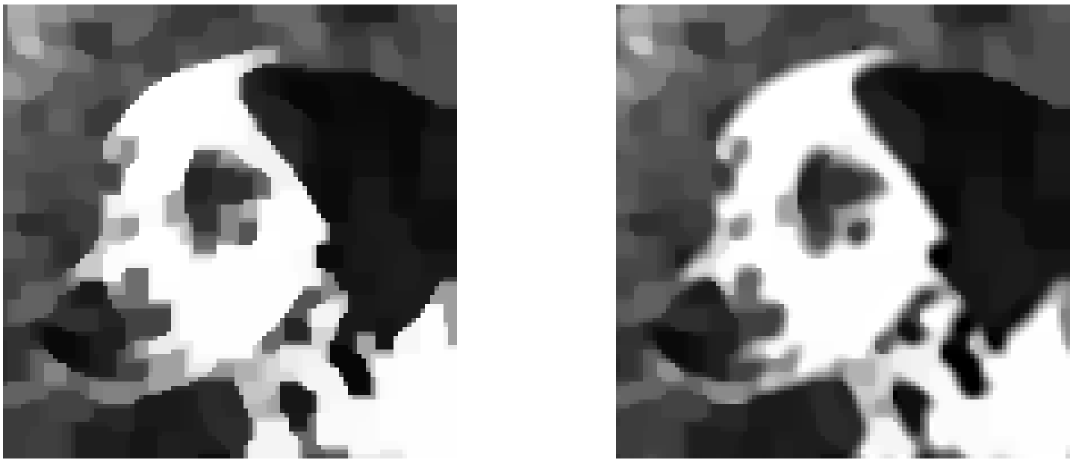

Figure 3: (a) Isotropic BV restoration; (b) Anisotropic BV restoration.

Finally, Figure 4 shows the restorations obtained with the mixed L^2-BV penalizer; isotropic case in (a) and anisotropic in (b).

(a) (b)

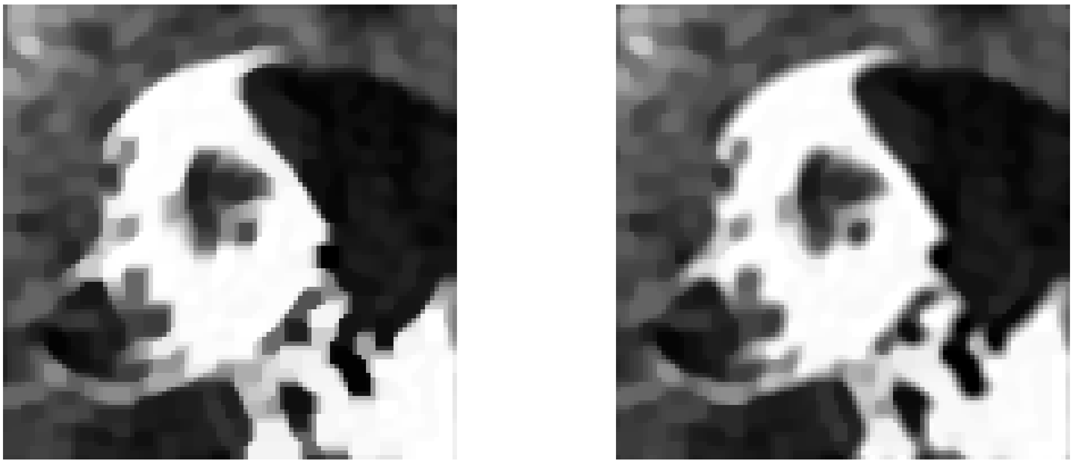

Figure 4: (a) Mixed L^2-isotropic BV restoration; (b) Mixed L^2-anisotropic BV restoration.

For comparison purposes, the original image is presented in Figure 5 and all ISNR values in Table 2. Once again, the best restoration is obtained with the combined L^2-anisotropic BV penalizer. It is also timely to see that the ISNR value of the anistropic BV restoration is significantly larger than the one obtained with the isotropic BV penalizer. Also, the ISNR increases from any one of the single methods to the corresponding combined one (namely, isotropic BV to mixed isotropic and anisotropic BV to mixed anisotropic). These observations clearly highlight the relevance and potential applications of the combined methods.

Figure 5: Original image

Restoration Type	ISNR
Tikhonov	4.140
Isotropic BV	3.666
Anisotropic BV	5.032
Mixed Isotropic	4.517
Mixed Anisotropic	5.118

Table 1: ISNRs of each restoration

4.2.2 A color image

Finally we present an application to a color image restoration problem. Here the forward model consists of applying the integral operator given by equation (27) to each one of the three layers (RGB) of the image. Blurring, noise contamination and restoration were all performed separately on each one of the layers. Figure 6(a) shows the blurred-noisy image (data) while Figure 6(b) shows the restoration obtained with a Tikhonov-Phillips (pure L^2) regularization method. Here too this restoration was used to build the anisotropic penalization matrices A_m and the components θ_m of the convex combination vector.

Figure 7 shows the restorations obtained with pure BV penalization terms, both isotropic (a) and anisotropic (b). The difference between the restorations induced by taking into account gradient-induced directions stands out clearly. Finally, Figure 8 shows the restorations performed with mixed L^2-BV regularization.

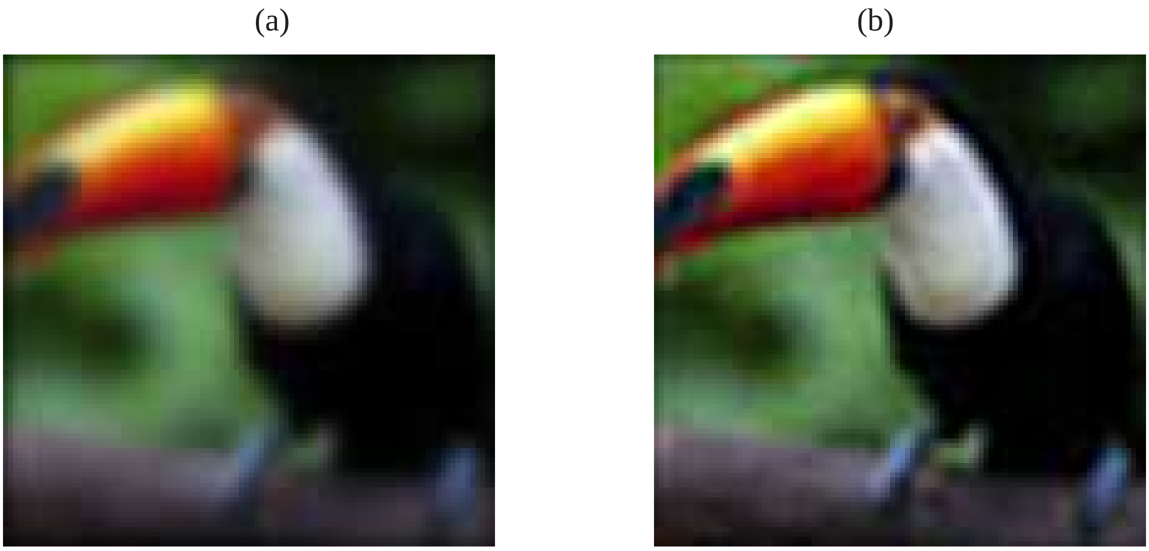

Figure 6: (a) Blurred noisy image (observation); (b) Tikhonov-Phillips restoration.

(a) (b)

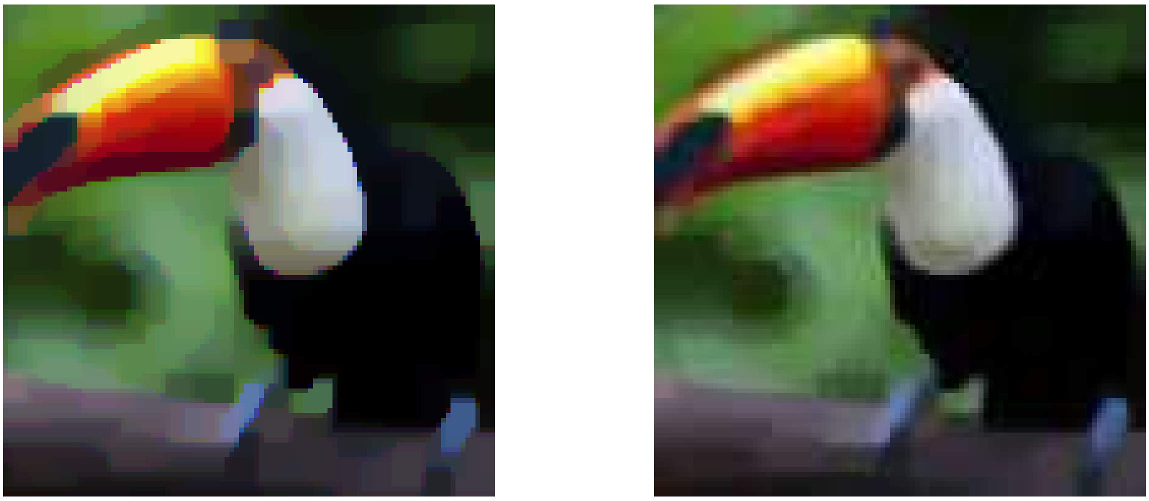

Figure 7: (a) Isotropic BV restoration; (b) Anisotropic BV restoration.

(a) (b)

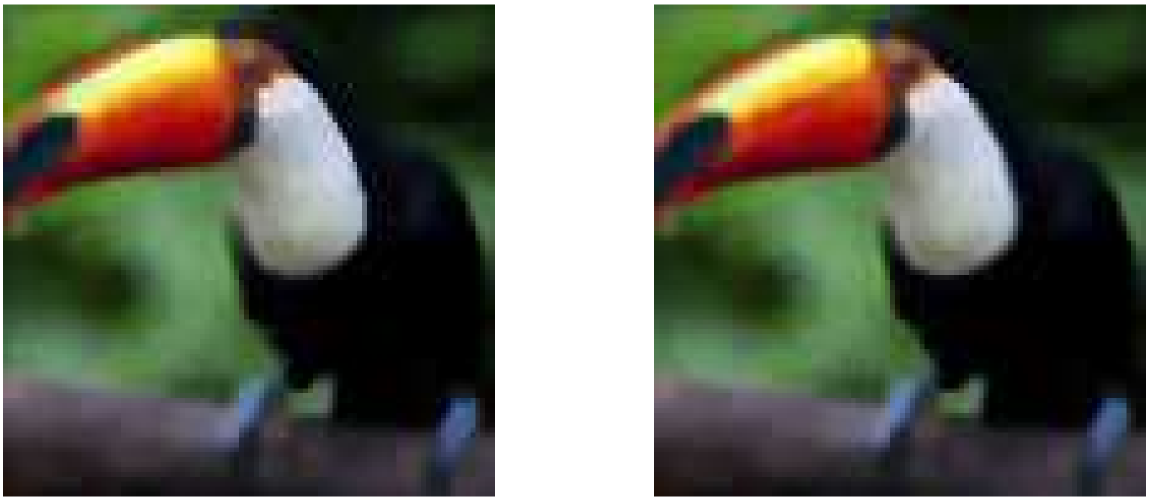

Figure 8: (a) Mixed L^2-isotropic BV restoration; (b) Mixed L^2-anisotropic BV restoration.

To better illustrate and compare the performances of the methods, Figure 9 shows the original image while Table 2 shows the ISNR values for each one of the five restorations.

Figure 9: Original image

Restoration Type	ISNR
Tikhonov	3.325
Isotropic BV	3.104
Anisotropic BV	4.042
Mixed Isotropic	3.846
Mixed Anisotropic	4.420

Table 2: ISNRs of each restoration

Similar observations as for the gray-scale example can be made here. Namely, the best restoration is once again obtained with the combined L^2-anisotropic BV penalizer, the ISNR value of the anistropic BV restoration is considerably larger than the one for the isotropic BV penalizer and the ISNR values increase from any one of the single methods to the corresponding combined one. For the sake of completness the next table shows the values of the regularization parameters λ_0 and λ_1 use for all previous restorations.

Restoration	Signal	Gray image	Red layer	Green layer	Blue layer
Tikhonov	1e-2	1e-2	1.42e-2	1.28e-2	1.56e-2
Isotropic BV	6.4e-4	7e-5	1.1e-4	1.2e-4	1e-4
Anisotropic BV	—	1e-4	1e-4	1.1e-4	1e-4
Mixed Isotropic	1.01e-2, 6.46e-4	8.59e-3, 6.01e-6	1.32e-4, 9e-5	1.12e-4, 1.1e-4	1.56e-2, 1e-4
Mixed Anisot.	—	1e-2, 1e-4	1.42e-2, 1.1e-4	1.28e-4, 1.2e-4	1.91e-2, 1.2e-4

Table 3: Values of the parameters λ_0 and λ_1 used for the different restorations

5 CONCLUSIONS

In this article we used a non-convex reformulation plus a non-quadratic half-quadratic approach to attack a general Tikhonov-Phillips regularization method were the penalizers are given by mixed spatially varying weighted convex combinations of L^2 and BV functionals. Both isotropic and anisotropic BV diffusion were considered. The associated optimization problems were then recast by means of a duality argument as half-quadratic optimization problems. The method proposed in this article resulted in significantly faster algorithms as compared to direct Newton-based methods. Numerical results in signal and image restoration problems were shown along with their ISNRs, whose higher values for the mixed-anisotropic restorations showed substantial improvements.

ACKNOWLEDGEMENTS

This work was supported in part by Agencia Nacional de Promoción Científica y Tecnológica, ANPCyT, through project PICT 2008-1301, by Universidad Nacional del Litoral, through projects CAI+D PJov 2011 Nro. 50020110100055, CAI+D PI 2011 Nro. 50120110100294 and by the Air Force Office of Scientific Research, AFOSR, through Grant FA9550-14-1-0130.

REFERENCES

Acar R. and Vogel C.R. Analysis of bounded variation penalty methods for ill-posed problems. *Inverse Problems*, 10:1217–1229, 1994.

Blomgren P., Chan T.F., Mulet P., and Wong C. Total variation image restoration: Numerical methods and extensions. *Proceedings of the IEEE International Conference on Image Processing*, III:384–387, 1997.

Calvetti D., Sgallari F., and Somersalo E. Image inpainting with structural boostrap priors. *Image and Vision Computing*, 24:782–793, 2006.

Chambolle A. and Lions J.L. Image recovery via total variation minimization and related problems. *Numer. Math.*, 76:167–188, 1997.

Chen Y., Levine S., and Rao M. Variable exponent, linear growth functionals in image restoration. *SIAM Journal Applied on Mathematics*, 66(4):1383–1406, 2006.

Engl H.W., Hanke M., and Neubauer A. *Regularization of inverse problems*, volume 375 of *Mathematics and its Applications*. Kluwer Academic Publishers Group, Dordrecht, 1996.

Hadamard J. Sur les problèmes aux dérivées partielles et leur signification physique. *Princeton University Bulletin*, 13:49–52, 1902.

Idier J. *Bayesian Approach to Inverse Problems*. John Wiley & Sons, 2008.

Li F., Li Z., and Pi L. Variable exponent functionals in image restoration. *Applied Mathematics and Computation*, 216:870–882, 2010.

Mazzieri G.L., Spies R.D., and Temperini K.G. Existence, uniqueness and stability of minimizers of generalized Tikhonov-Phillips functionals. *Journal of Mathematical Analysis and Applications*, 396:396–411, 2012.

Mazzieri G.L., Spies R.D., and Temperini K.G. Mixed spatially varying L^2-BV regularization of inverse ill-posed problems. *Journal of Inverse and Ill-posed Problems (submitted 2014) ArXiv:1403.5579v1 [math.FA] 21 Mar 2014, http://arxiv.org/abs/1403.5579v1*, 2014a.

Mazzieri G.L., Spies R.D., and Temperini K.G. Regularization of inverse ill-posed problems by anisotropic L^2-BV penalization. *In preparation*, 2014b.

Phillips D.L. A technique for the numerical solution of certain integral equations of the first kind. *J. Assoc. Comput. Mach.*, 9:84–97, 1962. ISSN 0004-5411.

Rockafellar R. *Convex Analysis*. Princeton University Press, 1970.

Rudin L.I., Osher S., and E. F. Nonlinear total variation based noise removal algorithms (proceedings of the 11th annual international conference of the center for nonlinear studies). *Physica D*, 60:259–268, 1992.

Spies R.D. and Temperini K.G. Arbitrary divergence speed of the least-squares method in infinite-dimensional inverse ill-posed problems. *Inverse Problems*, 22:611–626, 2006.

Tikhonov A.N. Solution of incorrectly formulated problems and the regularization method. *Soviet Math. Dokl.*, 4:1035–1038, 1963.